

B anomalies in the post $R_{K^{(*)}}$ era

T. Hurth^a, F. Mahmoudi^{b,c,d}, S. Neshatpour^{b,e}

^a*PRISMA+ Cluster of Excellence and Institute for Physics (THEP),
Johannes Gutenberg University, D-55099 Mainz, Germany*

^b*Université de Lyon, Université Claude Bernard Lyon 1, CNRS/IN2P3,
Institut de Physique des 2 Infinis de Lyon, UMR 5822, F-69622, Villeurbanne, France*

^c*CERN, Theoretical Physics Department, CH-1211 Geneva 23, Switzerland,*

^d*Institut Universitaire de France (IUF),*

^e*INFN-Sezione di Napoli, Complesso Universitario di Monte S. Angelo,
Via Cintia Edificio 6, 80126 Napoli, Italy*

ABSTRACT

We discuss the status of $b \rightarrow s\ell^+\ell^-$ decays in the post- $R_{K^{(*)}}$ era. The recent LHCb update of R_K and R_{K^*} measurements which are now compatible with the Standard Model, constrain new physics contributions to be lepton flavor universal, allowing only small deviations from this limit. Besides the latest LHCb measurements of R_K and R_{K^*} , we also include the recent CMS measurements of R_K and of the branching ratio of $B^+ \rightarrow K^+\mu^+\mu^-$. We present a model-independent analysis of the $b \rightarrow s\ell^+\ell^-$ data and investigate the implications of the different sets of observables. In addition, we consider multi-dimensional fits and discuss the significance of more complex new physics scenarios compared to one- and two-dimensional scenarios.

1 Introduction

Over the last nine years the LHCb collaboration reported hints for lepton non-universality at the 3σ level via measurements of the ratios R_K and R_{K^*} (see [1, 2] and references therein). The R_K and R_{K^*} which are defined as the ratios of the branching fractions of $B \rightarrow K^{(*)}\ell^+\ell^-$ for muons vs. electrons are theoretically very clean, with uncertainties of less than one percent and central values close to unity in the Standard Model (SM) due to the universality of the lepton flavours [3, 4]. In addition, there are long-standing tensions in the angular observables and branching ratios of exclusive $b \rightarrow s$ observables [5–13]. In general the observables of the exclusive decays are dependent on local matrix elements (form factors), as well as non-local ones which often make it difficult to distinguish between possible new physics effects and hadronic effects. Although some of the angular observables are less sensitive to the form factors, they do depend on non-local hadronic contributions, which are not well known. The significance of the anomalies in exclusive decays is therefore dependent on the estimated size of the non-local effects. Recent theoretical progress in the evaluation of the non-local contributions [14–16] indicate that the non-factorisable power corrections are small. The crucial point of the previous situation was that the deviations in the theoretically clean ratios on one side and in the angular observables and branching ratios on the other side could be consistently described with the same new physics scenarios. This consistency was again increased with the updated measurement of $\text{BR}(B_s \rightarrow \mu^+\mu^-)$ from last year [17]. The combination of this result with the ATLAS and LHCb measurements [18–20], $\text{BR}(B_s \rightarrow \mu^+\mu^-)_{\text{exp}}^{\text{comb.}} = (3.52_{-0.30}^{+0.32}) \times 10^{-9}$ as given in [21] is in agreement with the SM within 1σ , suppressing large new physics contributions in the Wilson coefficient C_{10} . However, the LHCb collaboration recently presented new measurements of the ratios which turn out to be compatible with the Standard Model [22]

$$\begin{cases} R_K([0.1 - 1.1]) = 0.994_{-0.082}^{+0.090} {}_{-0.027}^{+0.029}, & R_{K^*}([0.1 - 1.1]) = 0.927_{-0.087}^{+0.093} {}_{-0.035}^{+0.036}, \\ R_K([1.1 - 6.0]) = 0.949_{-0.041}^{+0.042} {}_{-0.022}^{+0.022}, & R_{K^*}([1.1 - 6.0]) = 1.027_{-0.068}^{+0.072} {}_{-0.026}^{+0.027}. \end{cases}$$

In this paper, we analyse the current situation in a model-independent way. Clearly, the tensions in the angular observables and branching ratios are untouched by the new LHCb measurements. We analyse the two sets of $b \rightarrow s$ data separately, namely the theoretically clean ratios together with $\text{BR}(B_{s,d} \rightarrow \ell^+\ell^-)$ on one side and the angular observables and branching ratios on the other side.

We also include the very recent measurements of R_K and the branching ratio of $B^+ \rightarrow K^+\mu^+\mu^-$ by the CMS collaboration [23], which both turn out to be compatible with the SM predictions. In addition, we update the CKM parameters where we have updated the PDG 2020 [24] values to PDG 2022 [25], with the old and new inputs given below

	λ	A	$\bar{\rho}$	$\bar{\eta}$
PDG (2020)	0.22650 ± 0.00048	$0.790_{-0.012}^{+0.017}$	$0.141_{-0.017}^{+0.016}$	0.357 ± 0.011
PDG (2022)	0.22500 ± 0.00067	$0.826_{-0.015}^{+0.018}$	0.159 ± 0.010	0.348 ± 0.010

The complete list of the observables used in the present fits can be read off the corresponding list in our previous analysis in Refs. [21, 26]. For our analysis we have used the SuperIso public program [27–31] assuming 10% uncertainty for the unknown non-factorisable power corrections (see Ref. [32] for more details). For other global analyses with the updated LHCb measurement of $R_{K^{(*)}}$ (not including the recent CMS measurement) see for example [33–35].

This paper is organised as follow, in the next section we show the one- and two-dimensional fits for different sets of observables. In section 2.1 we consider clean observables and discuss the impact of new LHCb measurement for the ratios, and in section 2.2 the fit to the rest of the observables are given where the impact from the CMS measurement on $\text{BR}(B^+ \rightarrow K^+ \mu^+ \mu^-)$ as well as the updated CKM values are visible. In section 2.3 the fit to all $b \rightarrow s$ data are given and the impact of various sets of observables are discussed. Section 3 includes a 12-dimensional fit and shows via the Wilks’ test that beyond C_9 adding further degrees of freedom only improves the fit marginally. Finally, we summarise in section 4.

2 One- and two-dimensional fits

2.1 Fits to clean $b \rightarrow s\ell\ell$ observables

Only LFUV ratios and $B_{s,d} \rightarrow \ell^+ \ell^-$ pre-$R_{K^{(*)}}$ update ($\chi_{\text{SM}}^2 = 30.63$)				Only LFUV ratios and $B_{s,d} \rightarrow \ell^+ \ell^-$ post-$R_{K^{(*)}}$ update ($\chi_{\text{SM}}^2 = 9.37$)			
	b.f. value	χ_{min}^2	Pull _{SM}		b.f. value	χ_{min}^2	Pull _{SM}
δC_9^e	0.83 ± 0.21	10.8	4.4σ	δC_9^e	0.17 ± 0.16	8.2	1.1σ
δC_9^μ	-0.80 ± 0.21	11.8	4.3σ	δC_9^μ	-0.18 ± 0.16	8.1	1.1σ
δC_{10}^e	-0.81 ± 0.19	8.7	4.7σ	δC_{10}^e	-0.15 ± 0.14	8.3	1.1σ
δC_{10}^μ	0.50 ± 0.14	16.2	3.8σ	δC_{10}^μ	0.15 ± 0.12	7.7	1.3σ
δC_{LL}^e	0.43 ± 0.11	9.7	4.6σ	δC_{LL}^e	0.08 ± 0.08	8.2	1.1σ
δC_{LL}^μ	-0.33 ± 0.08	12.4	4.3σ	δC_{LL}^μ	-0.09 ± 0.07	7.7	1.3σ

Table 1: One operator NP fit to clean observables before and after update of $R_{K^{(*)}}$ by the LHCb collaboration.

First, we analyse the significance of new physics (NP) within the clean observables, $R_{K^{(*)}}$ and $\text{BR}(B_{s,d} \rightarrow \mu^+ \mu^-)$. In Table 1 we show the one-operator fits to these clean observables, both before¹ and after the latest $R_{K^{(*)}}$ measurements. The change is a drastic one, as only small deviations from lepton-universality are now allowed. There are still lepton flavour universality violating (LFUV) ratios, namely $R_{K_S^0}^{\text{LHCb}}([1.1 - 6.0])$,

¹In this paper, pre- $R_{K^{(*)}}$ indicates the fit to the data before the LHCb update on $R_{K^{(*)}}$ as given in [21].

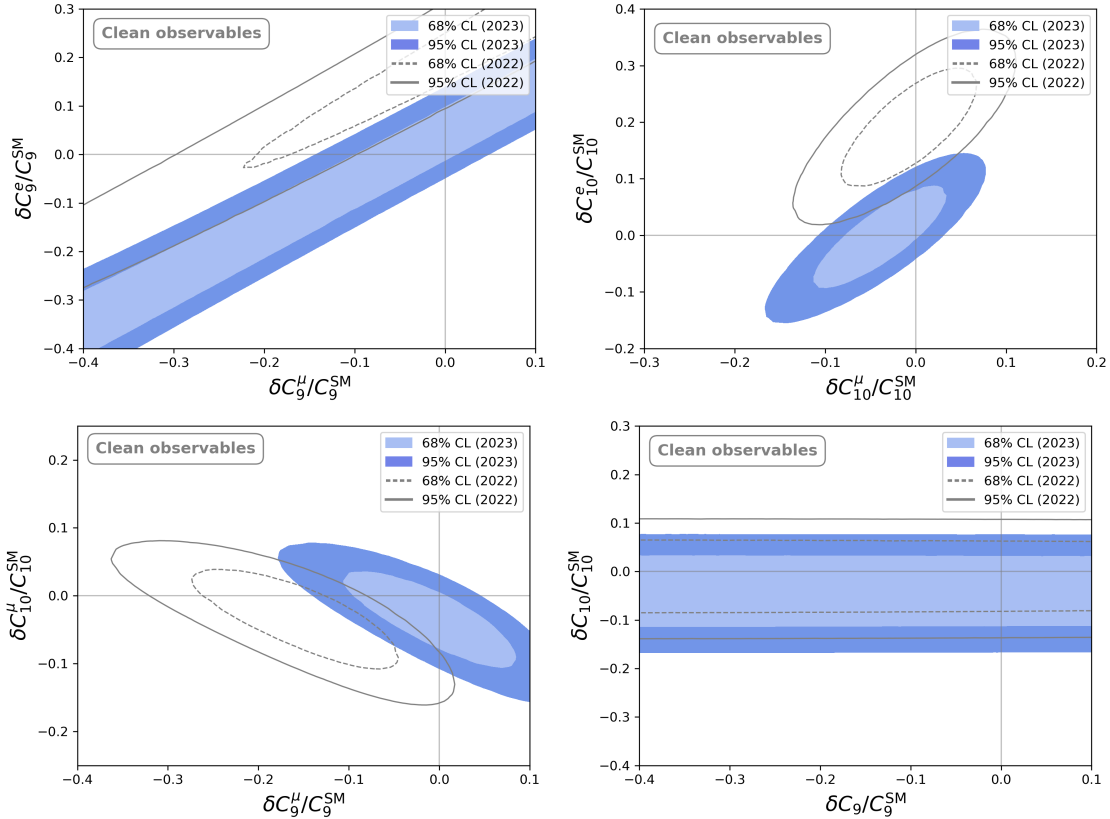


Figure 1: Two-dimensional fits to clean observables. The coloured regions correspond to the post- $R_{K^{(*)}}$ fits and the gray contours correspond to the fits prior to the recent $R_{K^{(*)}}$ update [21].

$R_{K^{*+}}^{\text{LHCb}}([0.045 - 6.0])$ [36] and $R_K^{\text{LHCb}}([1.1 - 6.0])$ [22] with 1.7, 1.4 and 1.1 σ NP significance, respectively.²

The corresponding two-operator fits are shown in Figure 1. The two upper plots clearly show that the new data confirms lepton universality. The 1 and 2 σ regions in the case of $\{C_9^e, C_9^\mu\}$ and also in the case of $\{C_{10}^e, C_{10}^\mu\}$ are located around the diagonal. The favoured regions in the case of $\{C_{10}^e, C_{10}^\mu\}$ are bounded along the diagonal because we have included $\text{BR}(B_{s,d} \rightarrow \mu^+ \mu^-)$ in the fit which implies strong constraints on C_{10} in general. The lower left plot in Figure 1 shows the two-operator fit to $\{C_9^\mu, C_{10}^\mu\}$. The 1 or 2 σ regions are now also grouped around the secondary diagonal and contain the SM values. Only small NP contributions are still possible after the new measurements. We note however that without $\text{BR}(B_{s,d} \rightarrow \mu^+ \mu^-)$ in the fit, i.e. without the strong constrain on C_{10}^μ much larger values of C_9^μ and C_{10}^μ would be possible along the secondary diagonal. Such larger contributions are then in principle possible but due to unnatural cancellations of these two contributions in the ratios R_K and R_{K^*} only. The lower right plot is trivial. It shows that our set of clean

²A re-analysis of $R_{K_S^0}^{\text{LHCb}}([1.1 - 6.0])$ and $R_{K^{*+}}^{\text{LHCb}}([0.045 - 6.0])$ regarding possible misidentifications would not change the NP significances much given the large experimental uncertainties [37].

observables does not constrain the universal coefficient C_9 , but that $\text{BR}(B_{s,d} \rightarrow \mu^+ \mu^-)$ constrains the universal C_{10} . The slight shift along the C_{10} axis compared to pre- $R_{K^{(*)}}$ fit is due to the modified SM prediction of $\text{BR}(B_s \rightarrow \mu^+ \mu^-)$ owing to the updated CKM inputs.

2.2 Fits to all $b \rightarrow s \ell \ell$ data except clean observables

All observables except LFUV ratios and $B_{s,d} \rightarrow \ell^+ \ell^-$ pre-$R_{K^{(*)}}$ update ($\chi_{\text{SM}}^2 = 221.8$)				All observables except LFUV ratios and $B_{s,d} \rightarrow \ell \bar{\ell}$ post-$R_{K^{(*)}}$ update ($\chi_{\text{SM}}^2 = 261.6$)			
	b.f. value	χ_{min}^2	Pull _{SM}		b.f. value	χ_{min}^2	Pull _{SM}
δC_9	-0.95 ± 0.13	185.1	6.1σ	δC_9	-0.97 ± 0.13	221.9	6.3σ
δC_9^e	0.70 ± 0.60	220.5	1.1σ	δC_9^e	0.70 ± 0.60	260.4	1.1σ
δC_9^μ	-0.96 ± 0.13	182.8	6.2σ	δC_9^μ	-0.98 ± 0.13	219.7	6.5σ
δC_{10}	0.29 ± 0.21	219.8	1.4σ	δC_{10}	0.36 ± 0.20	258.3	1.8σ
δC_{10}^e	-0.60 ± 0.50	220.6	1.1σ	δC_{10}^e	-0.50 ± 0.50	260.5	1.0σ
δC_{10}^μ	0.35 ± 0.20	218.7	1.8σ	δC_{10}^μ	0.41 ± 0.20	257.0	2.1σ
δC_{LL}^e	0.34 ± 0.29	220.6	1.1σ	δC_{LL}^e	0.31 ± 0.28	260.4	1.1σ
δC_{LL}^μ	-0.64 ± 0.13	195.0	5.2σ	δC_{LL}^μ	-0.65 ± 0.12	231.7	5.5σ

Table 2: One operator fits for all except clean observables before (left) and also after (right) the LHCb-update of $R_{K^{(*)}}$.

In Table 2 we show the one-parameter fits to the rest of the $b \rightarrow s$ observables - excluding the clean observables discussed before. These fits are of course almost unchanged compared to the situation before the new measurements of R_K and R_{K^*} . The slight differences in the NP significance are due to the new measurements by CMS and also update of the CKM parameters. But the comparison of the one-operator fits to the clean observables in Table 1 and of those to the remaining $b \rightarrow s$ observables in Table 2 shows for the non-universal Wilson coefficients C_9^μ and C_{LL}^μ no longer any consistency, which means that the remaining large tensions in the rest of the $b \rightarrow s$ observables, in particular in the angular observables and in the branching ratios, should be described with lepton-universal operators, only small deviations from the lepton universality are allowed. Let us emphasise that the NP significances given in Table 2 are based on the assumption of 10% power corrections to the angular observables and branching ratios.

2.3 Fits to all $b \rightarrow s \ell \ell$ observables

This brings us to the fits to all $b \rightarrow s$ observables where we now use lepton-universal operators only – assuming again 10% power corrections for the angular observables and branching ratios. The results are given in Table 3 where we can see that the favoured universal coefficient is C_9 in order to explain the tensions in the angular observables and branching ratios. In principle, C_9^μ and C_{LL}^μ can explain the tensions but these new physics

contributions would not be compatible with the constraints induced by the clean observables as we showed above. In Table 4 one operator fits using chiral universal coefficients³ are shown. One finds a rather large NP significance for the fits to C_{LL} and C_{LR} , i.e. for left-handed quark currents.

All observables pre-$R_{K^{(*)}}$ update ($\chi_{\text{SM}}^2 = 253.5$)				All observables post-$R_{K^{(*)}}$ update ($\chi_{\text{SM}}^2 = 271.0$)			
	b.f. value	χ_{min}^2	Pull _{SM}		b.f. value	χ_{min}^2	Pull _{SM}
δC_7	-0.02 ± 0.01	248.7	2.2σ	δC_7	-0.02 ± 0.01	267.2	1.9σ
δC_{Q_1}	-0.05 ± 0.02	252.3	1.1σ	δC_{Q_1}	-0.04 ± 0.03	270.3	0.8σ
δC_{Q_2}	-0.01 ± 0.01	252.4	1.0σ	δC_{Q_2}	-0.01 ± 0.01	270.4	0.8σ
δC_9	-0.95 ± 0.13	215.8	6.1σ	δC_9	-0.96 ± 0.13	230.7	6.3σ
δC_{10}	0.08 ± 0.16	253.2	0.5σ	δC_{10}	0.15 ± 0.15	270.0	1.0σ

Table 3: One operator NP fits to all $b \rightarrow s\ell\ell$ observables before and after the update of $R_{K^{(*)}}$ by the LHCb collaboration.

All observables post-$R_{K^{(*)}}$ update ($\chi_{\text{SM}}^2 = 271.0$)			
	b.f. value	χ_{min}^2	Pull _{SM}
δC_{LL}	-0.54 ± 0.12	249.1	4.7σ
δC_{LR}	-0.42 ± 0.10	257.4	3.7σ
δC_{RL}	0.00 ± 0.08	268.8	1.5σ
δC_{RR}	0.21 ± 0.13	268.1	1.7σ

Table 4: One operator fits to all $b \rightarrow s\ell\ell$ observables in the chiral basis.

In addition, we present the two-dimensional fit results in Figure 2. The lower right plot in the $\{C_9, C_{10}\}$ plane is the crucial one. It shows that not the universal coefficient C_{10} but C_9 explains the present anomalies best. This is also a consequence of the C_{10} dependence of the $B_s \rightarrow \mu^+\mu^-$ branching ratio which is SM-like. The two-operator fits in the upper row, $\{C_9^\mu, C_9^e\}$ and $\{C_{10}^\mu, C_{10}^e\}$, essentially are again consequences of lepton-flavour universality. In both plots, the 1 and 2σ ranges have move to the diagonal and have become thinner compared to the ones of the pre- $R_{K^{(*)}}$ measurements. Moreover, the 1σ range of $\{C_{10}^\mu, C_{10}^e\}$ fit includes the SM values. It becomes clear that these two-operator

³We use the standard notation: C_{XY} where X denotes the chirality of the quark current and Y of the lepton one. Assuming left-handed leptons only, we have $C_{LL} \equiv C_9 = -C_{10}$ and $C_{RL} \equiv C_9' = -C_{10}'$, for right-handed leptons $C_{RR} \equiv C_9' = C_{10}'$ and $C_{LR} \equiv C_9 = C_{10}$.

All observables post- $R_{K^{(*)}}$ update ($\chi_{\text{SM}}^2 = 271.0$)			
	b.f. value	χ_{min}^2	Pull _{SM}
$\{\delta C_9^\mu, \delta C_9^e\}$	$\{-0.96 \pm 0.13, -0.74 \pm 0.21\}$	228.8	6.2σ
$\{\delta C_{10}^\mu, \delta C_{10}^e\}$	$\{0.15 \pm 0.15, -0.03 \pm 0.21\}$	268.3	1.1σ
$\{\delta C_9^\mu, \delta C_{10}^\mu\}$	$\{-0.78 \pm 0.12, -0.19 \pm 0.10\}$	237.2	5.5σ
$\{\delta C_9, \delta C_{10}\}$	$\{-0.97 \pm 0.13, 0.09 \pm 0.15\}$	230.3	6.0σ

Table 5: Two operator NP fits to all observables (post- $R_{K^{(*)}}$ update). The corresponding plots are given in Fig. 2.

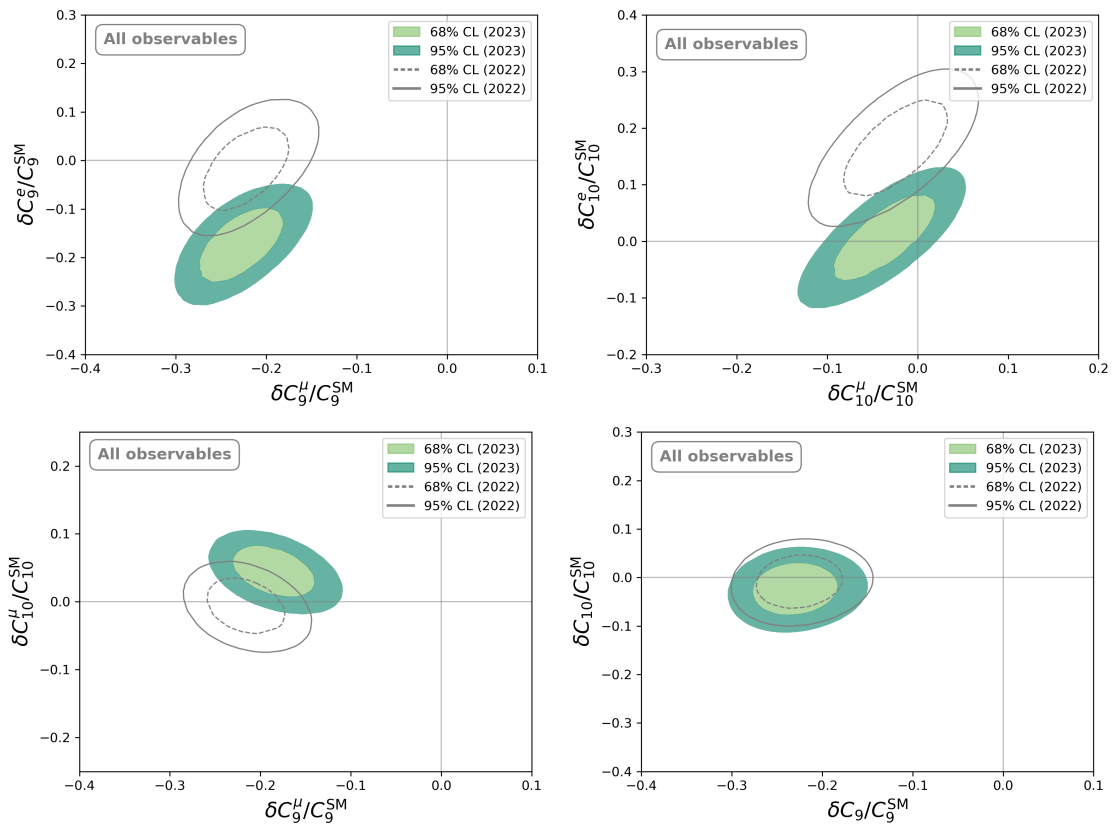


Figure 2: Two-dimensional fits to all observables with the best-fit point given in Table 5.

plots essentially reproduce the one-operator fits to the corresponding universal C_9 and C_{10} . Also the NP significance is similar as one can read off from Tables 3 and 5.

The plot in the lower row on the left shows the two-operator fit to $\{C_9^\mu, C_{10}^\mu\}$. Compared to the pre- $R_{K^{(*)}}$ update, the 1 or 2σ ranges now move in the direction of the second diagonal to allow a partial compensation of the C_9^μ and the C_{10}^μ contributions within the $R_{K^{(*)}}$ ratios. Because of this unnatural compensation, this specific two-operator fit should be considered

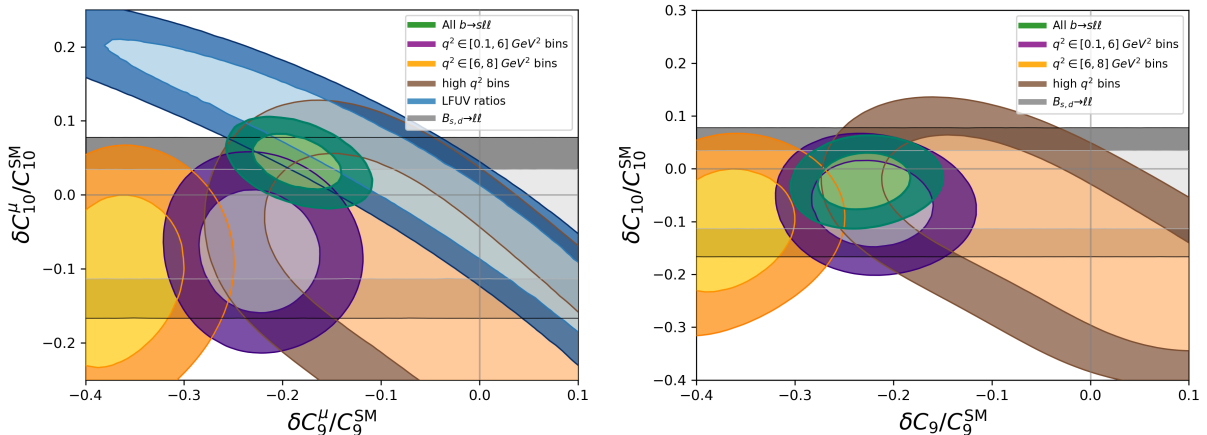


Figure 3: Two-dimensional fits to all observables in green. Where relevant, the impact of the $b \rightarrow s\ell\ell$ observables for the low q^2 bins up to 6 GeV², for the [6, 8] GeV² bin and for the high q^2 bins as well as the bounds from the lepton flavour universality violating ratios and $B_{s,d} \rightarrow \ell^+\ell^-$ are shown separately with the lighter (darker) shade indicating the 68% (95%) confidence level region.

critical. In comparison with the corresponding plot in Figure 1 with the fits to the clean observables, one needs now a larger C_9^μ for the explanation of the present tensions which again indicates the present measurements are best described by flavour-universal operators.

As one can read off from Table 5, all two-operator fits discussed have a large NP significance up to 6σ besides the case $\{C_{10}^\mu, C_{10}^e\}$.

Next, we will have a closer look at the two two-operator fits to $\{C_9^\mu, C_{10}^\mu\}$ and $\{C_9, C_{10}\}$. We consider the bounds of the $R_{K^{(*)}}$ ratios separately from the ones induced by the $B_{s,d} \rightarrow \mu^+\mu^-$ branching ratios. Likewise, in the case of the remaining $b \rightarrow s\ell^+\ell^-$ observables, we examine the impact of the low- q^2 and the high- q^2 observables separately. Since the validity of SCET in the low- q^2 bin [6, 8] GeV² (near the J/ψ resonance) is questionable, we separate this bin from the other low- q^2 bins up to 6 GeV².

In Figure 3 the two-operator fits have been dissected in order to show the impact that each of these different sets of observables have on the overall fit. In the plot on the right hand side of Figure 3 the $\{C_9, C_{10}\}$ two-operator fit has been shown, where the brown contours show the 1 and 2σ regions of the high- q^2 observables. It can be seen that they are compatible with the SM values with comparatively large uncertainties. The tensions in the angular observables and the branching ratios obviously have their main origin in the low- q^2 observables as can be seen from the purple contours. It is well-known that the high- q^2 observables have a weak dependence on the Wilson coefficients, which implies a low sensitivity to NP.⁴ The yellow contours show that the inclusion of the highest low- q^2 bin from 6 to 8 GeV² in the fit massively increases the NP significance. However, it could be that this large effect just indicates that SCET is no longer valid in this range. Finally,

⁴In principle the high- q^2 observables are theoretically cleaner. There is a local operator product expansion (OPE) to describe power corrections (see i.e. Refs. [38, 39]).

All observables with $\chi_{\text{SM}}^2 = 271.0$ post-$R_{K^{(*)}}$ update ($\chi_{\text{min}}^2 = 222.5$; $\text{Pull}_{\text{SM}} = 4.7\sigma$)			
δC_7 0.07 ± 0.03		δC_8 -0.70 ± 0.50	
$\delta C'_7$ -0.01 ± 0.01		$\delta C'_8$ -0.50 ± 1.20	
δC_9 -1.18 ± 0.19	$\delta C'_9$ 0.06 ± 0.31	δC_{10} 0.23 ± 0.20	$\delta C'_{10}$ -0.05 ± 0.19
C_{Q_1} -0.30 ± 0.14	C'_{Q_1} -0.18 ± 0.14	C_{Q_2} 0.01 ± 0.02	C'_{Q_2} -0.03 ± 0.07

Table 6: The 12-dimensional (lepton flavour universal) fit to all observables.

the $B_{s,d} \rightarrow \mu^+ \mu^-$ branching ratios lead to the grey contours which just bound the Wilson coefficient C_{10} .

In the plot on the left hand side of Figure 3 we look at the bounds on $\{C_9^\mu, C_{10}^\mu\}$. The blue 1 and 2σ regions show the bounds generated by the ratios $R_{K^{(*)}}$. This can be compared to the lower right plot of Figure 1 where the bound from the ratios together with $\text{BR}(B_{s,d} \rightarrow \mu^+ \mu^-)$ was shown. One realises that now much larger values of C_9^μ and also of C_{10}^μ are allowed, but this is possible due to an unnatural compensation between the C_9^μ and the C_{10}^μ contributions in the ratios which makes the $\{C_9^\mu, C_{10}^\mu\}$ fit problematic, as already mentioned above. The $B_{s,d} \rightarrow \mu^+ \mu^-$ branching ratios alone bound C_{10}^μ to smaller values again, as can be seen from the grey contours.

3 Global analyses

In order to present the global analysis, we provide multi-dimensional fits considering only universal operators, which may be more realistic than assuming one- or two-operator fits, since it is unlikely that a complete NP scenario would affect only one parameter while leaving the others unchanged. We therefore consider a fit varying simultaneously all the relevant 12 lepton-flavour universal Wilson coefficients. This multi-dimensional fit also avoids the look-elsewhere effect (LEE), which can occur when making a selected choice of observables or when assuming a subset of specific new physics directions. The results are presented in Table 6. As can be seen, most primed coefficients (with right-handed quark currents) are only loosely constrained with the currently available data. In Table 7 we compare the significance of different NP fits (all lepton-flavour universal) compared to the SM and to each other considering the Wilks' theorem [40]. Since the NP scenarios in Table 7 are nested in the model of the next row, we can calculate p -values using Wilks' theorem. The difference in χ^2 between the two models is itself a χ^2 -distribution with a number of degrees of freedom equal to the difference in the number of parameters. The

p -value therefore indicates the significance of the new parameters added. We have then converted these p -values to sigmas. From Table 7, it is clear that the main coefficient explaining the measured tensions in $b \rightarrow s$ decays is C_9 and beyond that adding further degrees of freedom does not improve the fit significantly. Thus, also the Wilks' test confirms the crucial role of C_9 for the explanation of the anomalies in the angular observables and branching ratios.

All observables (post-$R_{K^{(*)}}$ update)				
Set of WC	param.	χ^2_{\min}	Pull _{SM}	Improvement
SM	0	271.0	–	–
C_9	1	230.7	6.3σ	6.3σ
C_9, C_{10}	2	230.3	6.0σ	0.6σ
C_7, C_8, C_9, C_{10}	4	225.3	5.9σ	1.7σ
$C_7, C_8, C_9, C_{10}, C_{Q_1}, C_{Q_2}$	6	224.7	5.6σ	0.3σ
All WC (incl. primed)	12	222.5	4.7σ	0.1σ

Table 7: Pull_{SM} of 1, 2, 4, 6 and 12 dimensional fit. The last row includes all Wilson coefficients including the chirality-flipped primed coefficients. The last column indicates the significance of the improvement of the fit compared to the previous row.

4 Summary

In light of the recent LHCb measurement of R_K and R_{K^*} which is in agreement with the Standard Model (SM) prediction, we have analysed the current status of $b \rightarrow s$ semileptonic decays, including this new measurement, as well as the very recent measurement of R_K and $\text{BR}(B^+ \rightarrow K^+ \mu^+ \mu^-)$ by the CMS collaboration. We have also updated the CKM parameters to the PDG2022 values.

The clean observables R_K , R_{K^*} , and $\text{BR}(B_s \rightarrow \mu^+ \mu^-)$ are now all in good agreement with the SM. The ratios constrain new physics contributions in $b \rightarrow s \ell^+ \ell^-$ decays to be lepton flavour universal, with room for only small universality violating contributions while $\text{BR}(B_s \rightarrow \mu^+ \mu^-)$ constrains new physics contributions in the axial Wilson coefficient C_{10} . Furthermore, we showed that although the two-dimensional fit $\{C_9^\mu, C_{10}^\mu\}$ (with C_9^e and C_{10}^e kept to their SM values) indicates preference for NP in C_9^μ and to a lesser degree in C_{10}^μ , this two-operator fit should be viewed critically because it gives a LFUV solution which is at odds with the recent $R_{K^{(*)}}$ measurements.

However, the tensions in the angular observables and branching ratios are untouched by the new LHCb measurements. These tensions are best explained by a lepton flavour universal NP in the Wilson coefficient C_9 , which is mostly due to the low- q^2 observables, especially from the $[6 - 8] \text{ GeV}^2$ bin, keeping in mind that this latter on the one hand is more sensitive to C_9 contributions, and on the other hand more prone to being contaminated by charm-loop contributions. Moreover, as shown via the Wilks' test, new physics contributions in C_9 is the main scenario explaining the measured tensions in $b \rightarrow s$ decays

and there is no significant improvement in the fit when considering more complex models with additional degrees of freedom.

Acknowledgement

The authors are grateful to P. Owen for useful discussions. TH is supported by the Cluster of Excellence “Precision Physics, Fundamental Interactions, and Structure of Matter” (PRISMA+ EXC 2118/1) funded by the German Research Foundation (DFG) within the German Excellence Strategy (Project ID 39083149). SN was supported in part by the INFN research initiative Exploring New Physics (ENP).

References

- [1] LHCb collaboration, *Test of lepton universality with $B^0 \rightarrow K^{*0} \ell^+ \ell^-$ decays*, *JHEP* **08** (2017) 055 [[1705.05802](#)].
- [2] LHCb collaboration, *Test of lepton universality in beauty-quark decays*, *Nature Phys.* **18** (2022) 277 [[2103.11769](#)].
- [3] G. Hiller and F. Kruger, *More model-independent analysis of $b \rightarrow s$ processes*, *Phys. Rev. D* **69** (2004) 074020 [[hep-ph/0310219](#)].
- [4] M. Bordone, G. Isidori and A. Pattori, *On the Standard Model predictions for R_K and R_{K^*}* , *Eur. Phys. J. C* **76** (2016) 440 [[1605.07633](#)].
- [5] LHCb collaboration, *Measurement of Form-Factor-Independent Observables in the Decay $B^0 \rightarrow K^{*0} \mu^+ \mu^-$* , *Phys. Rev. Lett.* **111** (2013) 191801 [[1308.1707](#)].
- [6] LHCb collaboration, *Differential branching fractions and isospin asymmetries of $B \rightarrow K^{(*)} \mu^+ \mu^-$ decays*, *JHEP* **06** (2014) 133 [[1403.8044](#)].
- [7] LHCb collaboration, *Differential branching fraction and angular analysis of $\Lambda_b^0 \rightarrow \Lambda \mu^+ \mu^-$ decays*, *JHEP* **06** (2015) 115 [[1503.07138](#)].
- [8] LHCb collaboration, *Angular analysis and differential branching fraction of the decay $B_s^0 \rightarrow \phi \mu^+ \mu^-$* , *JHEP* **09** (2015) 179 [[1506.08777](#)].
- [9] LHCb collaboration, *Angular analysis of the $B^0 \rightarrow K^{*0} \mu^+ \mu^-$ decay using 3 fb^{-1} of integrated luminosity*, *JHEP* **02** (2016) 104 [[1512.04442](#)].
- [10] LHCb collaboration, *Measurement of CP-Averaged Observables in the $B^0 \rightarrow K^{*0} \mu^+ \mu^-$ Decay*, *Phys. Rev. Lett.* **125** (2020) 011802 [[2003.04831](#)].
- [11] LHCb collaboration, *Angular Analysis of the $B^+ \rightarrow K^{*+} \mu^+ \mu^-$ Decay*, *Phys. Rev. Lett.* **126** (2021) 161802 [[2012.13241](#)].

- [12] LHCb collaboration, *Angular analysis of the rare decay $B_s^0 \rightarrow \phi\mu^+\mu^-$* , *JHEP* **11** (2021) 043 [[2107.13428](#)].
- [13] LHCb collaboration, *Branching Fraction Measurements of the Rare $B_s^0 \rightarrow \phi\mu^+\mu^-$ and $B_s^0 \rightarrow f_2'(1525)\mu^+\mu^-$ Decays*, *Phys. Rev. Lett.* **127** (2021) 151801 [[2105.14007](#)].
- [14] C. Bobeth, M. Chrzaszcz, D. van Dyk and J. Virto, *Long-distance effects in $B \rightarrow K^*\ell\ell$ from analyticity*, *Eur. Phys. J. C* **78** (2018) 451 [[1707.07305](#)].
- [15] N. Gubernari, D. van Dyk and J. Virto, *Non-local matrix elements in $B_{(s)} \rightarrow \{K^{(*)}, \phi\}\ell^+\ell^-$* , *JHEP* **02** (2021) 088 [[2011.09813](#)].
- [16] N. Gubernari, M. Reboud, D. van Dyk and J. Virto, *Improved theory predictions and global analysis of exclusive $b \rightarrow s\mu^+\mu^-$ processes*, *JHEP* **09** (2022) 133 [[2206.03797](#)].
- [17] CMS collaboration, *Measurement of the $B_s^0\mu^+\mu^-$ decay properties and search for the $B^0 \rightarrow \mu^+\mu^-$ decay in proton-proton collisions at $\sqrt{s} = 13$ TeV*, *Phys. Lett. B* **842** (2023) 137955 [[2212.10311](#)].
- [18] ATLAS collaboration, *Study of the rare decays of B_s^0 and B^0 mesons into muon pairs using data collected during 2015 and 2016 with the ATLAS detector*, *JHEP* **04** (2019) 098 [[1812.03017](#)].
- [19] LHCb collaboration, *Measurement of the $B_s^0 \rightarrow \mu^+\mu^-$ decay properties and search for the $B^0 \rightarrow \mu^+\mu^-$ and $B_s^0 \rightarrow \mu^+\mu^-\gamma$ decays*, *Phys. Rev. D* **105** (2022) 012010 [[2108.09283](#)].
- [20] LHCb collaboration, *Analysis of Neutral B-Meson Decays into Two Muons*, *Phys. Rev. Lett.* **128** (2022) 041801 [[2108.09284](#)].
- [21] S. Neshatpour, T. Hurth, F. Mahmoudi and D. Martinez Santos, *Neutral Current B-Decay Anomalies*, *Springer Proc. Phys.* **292** (2023) 11 [[2210.07221](#)].
- [22] LHCb collaboration, *Measurement of lepton universality parameters in $B^+ \rightarrow K^+\ell^+\ell^-$ and $B^0 \rightarrow K^{*0}\ell^+\ell^-$ decays*, *Phys. Rev. D* **108** (2023) 032002 [[2212.09153](#)].
- [23] CMS collaboration, *Test of lepton flavor universality in $B^\pm \rightarrow K^\pm\ell^+\ell^-$ decays, CMS-PAS-BPH-22-005* (2023) .
- [24] PARTICLE DATA GROUP collaboration, *Review of Particle Physics*, *PTEP* **2020** (2020) 083C01.
- [25] PARTICLE DATA GROUP collaboration, *Review of Particle Physics*, *PTEP* **2022** (2022) 083C01.

- [26] T. Hurth, F. Mahmoudi, D.M. Santos and S. Neshatpour, *More Indications for Lepton Nonuniversality in $b \rightarrow s\ell^+\ell^-$* , *Phys. Lett. B* **824** (2022) 136838 [[2104.10058](#)].
- [27] F. Mahmoudi, *SuperIso: A Program for calculating the isospin asymmetry of $B \rightarrow K^*\gamma$ in the MSSM*, *Comput. Phys. Commun.* **178** (2008) 745 [[0710.2067](#)].
- [28] F. Mahmoudi, *SuperIso v2.3: A Program for calculating flavor physics observables in Supersymmetry*, *Comput. Phys. Commun.* **180** (2009) 1579 [[0808.3144](#)].
- [29] F. Mahmoudi, *SuperIso v3.0, flavor physics observables calculations: Extension to NMSSM*, *Comput. Phys. Commun.* **180** (2009) 1718.
- [30] S. Neshatpour and F. Mahmoudi, *Flavour Physics with SuperIso*, *PoS TOOLS2020* (2021) 036 [[2105.03428](#)].
- [31] S. Neshatpour and F. Mahmoudi, *Flavour Physics Phenomenology with SuperIso*, *PoS CompTools2021* (2022) 010 [[2207.04956](#)].
- [32] T. Hurth, F. Mahmoudi and S. Neshatpour, *On the anomalies in the latest LHCb data*, *Nucl. Phys. B* **909** (2016) 737 [[1603.00865](#)].
- [33] M. Algueró, A. Biswas, B. Capdevila, S. Descotes-Genon, J. Matias and M. Novoa-Brunet, *To (b)e or not to (b)e: no electrons at LHCb*, *Eur. Phys. J. C* **83** (2023) 648 [[2304.07330](#)].
- [34] M. Ciuchini, M. Fedele, E. Franco, A. Paul, L. Silvestrini and M. Valli, *Constraints on lepton universality violation from rare B decays*, *Phys. Rev. D* **107** (2023) 055036 [[2212.10516](#)].
- [35] A. Greljo, J. Salko, A. Smolkovič and P. Stangl, *Rare b decays meet high-mass Drell-Yan*, *JHEP* **05** (2023) 087 [[2212.10497](#)].
- [36] LHCb collaboration, *Tests of lepton universality using $B^0 \rightarrow K_S^0\ell^+\ell^-$ and $B^+ \rightarrow K^{*+}\ell^+\ell^-$ decays*, *Phys. Rev. Lett.* **128** (2022) 191802 [[2110.09501](#)].
- [37] P. Owen. Private communication.
- [38] C. Bobeth, G. Hiller and D. van Dyk, *The Benefits of $\bar{B} \rightarrow \bar{K}^*\ell^+\ell^-$ Decays at Low Recoil*, *JHEP* **07** (2010) 098 [[1006.5013](#)].
- [39] M. Beylich, G. Buchalla and T. Feldmann, *Theory of $B \rightarrow K^{(*)}\ell^+\ell^-$ decays at high q^2 : OPE and quark-hadron duality*, *Eur. Phys. J. C* **71** (2011) 1635 [[1101.5118](#)].
- [40] S.S. Wilks, *The Large-Sample Distribution of the Likelihood Ratio for Testing Composite Hypotheses*, *Annals Math. Statist.* **9** (1938) 60.